the distances involved are much too large. The bundles thus correspond to aggregates of molecules. The existence of superstructures and aggregates has been reported in a variety of polymer systems (although not in polystyrene at room temperature), especially those of biological importance, but the underlying cause of the aggregation is not clear (*18*). In our experiments, we were able to easily induce the formation of clumps of polystyrene molecules in the surface films; by understanding the origin of the time-dependent patterns we create while scanning the surface, we hope to learn more about this process of aggregation.

There are two interesting aspects of the pattern of structures formed in our experiments: (i) the uniformity of the structures makes the images appear periodic, and (ii) the bundles formed are elongated such that the long axis is perpendicular to the scan direction (*19*). We can check that the orientation of the bundles is indeed perpendicular to that of the scan direction by simply rotating the scan direction after several minutes. In this case we found that the direction of the bundles rotated as well.

As the tip was allowed to scan for a longer time, we observed that the aggregation process continued and that the bundles grew in size (Fig. 3A). From a comparison of Figs. 3B and 2E, it appears that the bundles that were distinct after 5 min of scanning had begun to aggregate to form larger bundles. These results are summarized in Fig. 4, which also shows that the polymer film did not aggregate simply as a result of the elapsed time. A smaller region (1.5 μm by 1.5 μm) was scanned continuously for 4 hours; then the scan size was increased to 6 μm by 6 μm, and this larger region was scanned for 5 min. The overall image was then taken at the first scan of the 10 μm by 10 μm area. The patterns formed are consistent with Figs. 2 and 3, and the boundaries between the regions are quite sharp.

Three conditions were necessary for the formation of surface structures: (i) there must be a reasonable balance between tip–surface molecule forces versus surface molecule–surface molecule forces, (ii) the deformation should be plastic, and (iii) there must be enough molecules on the surface. We realized these conditions in our experiments by using a polymer deposited onto a surface as a multilayer from a dilute solution. Because the polymer chains were weakly interacting in solution and the solvent evaporated rapidly, chains that were entangled but loosely bound were presumably formed at the surface. Otherwise, the tip-polymer interaction may not be strong enough to cause a deformation (*20*).

One of the interesting aspects about being able to produce these structures is the possibility of obtaining novel properties from the material. Although the maximum scan size of our AFM is 12 μm by 12 μm, by translating the sample and making further scans, we are able to produce macroscopic areas of aligned structures.

REFERENCES AND NOTES

1. G. Binnig, C. F. Quate, Ch. Gerber, *Phys. Rev. Lett.* **56**, 930 (1986).
2. C. M. Mate, G. M. McClelland, R. Erlandsson, S. Chiang, *ibid.* **59**, 1942 (1987).
3. R. Erlandsson, G. Hardzioannou, C. M. Mate, G. M. McClelland, S. Chiang, *J. Chem. Phys.* **89**, 5190 (1988).
4. N. A. Burnham and R. J. Colton, *J. Vac. Sci. Technol. A* **7**, 2906 (1989).
5. A. L. Weisenhorn, P. K. Hansma, T. R. Albrecht, C. F. Quate, *Appl. Phys. Lett.* **54**, 2651 (1989).
6. O. Marti *et al.*, *Science* **239**, 50 (1988).
7. B. N. Person, *Chem. Phys. Lett.* **141**, 366 (1987).
8. F. F. Abraham and I. P. S. Batra, *Surface Sci.* **209**, L125 (1989).
9. A number of recent studies in nanoscale manipulation of adsorbates on conducting surfaces have been done by scanning tunneling microscopy: L. J. Whitman, J. A. Stroscio, R. A. Dragoset, R. J. Celotta, *Science* **251**, 1206 (1991); D. M. Eigler and E. K. Schweizer, *Nature* **344**, 524 (1990); J. S. Foster, J. E. Frommer, P. C. Arnett, *ibid.* **331**, 324 (1988); R. S. Becker, J. A. Golovchenko, B. S. Swartzentruber, *ibid.* **325**, 419 (1987). These manipulations rely on the application of a voltage pulse to the tip.
10. U. Landman, W. D. Luedtke, N. A. Burnham, R. J. Colton, *Science* **248**, 454 (1990).
11. In dilute solutions, the polymer chains are well separated and noninteracting.
12. We also used toluene and chloroform as solvents; similar results were obtained.
13. We define the coordinates such that the z axis is perpendicular to the surface plane and the x axis is horizontal in all the images presented here.
14. We do not rule out the possibility that some polymer molecules may jump and coat the tip as well. (We found indirect evidence for this: after scanning the surface for a long time, the images get worse, but, if the tip is washed with a solvent that dissolves the polymer, it functions as well as a new tip.) However, there is enough polymer in the deposited film, and eventually the entanglement is expected to lead to the situation described.
15. The lump persisted for at least several hours. However, we were unable to follow the behavior for a longer time for technical reasons: if the sample is removed from the microscope, it is very difficult to find the location of a 10-nm structure within a sample 1 cm square.
16. L. H. Sperling, *Introduction to Polymer Science* (Wiley, New York, 1985).
17. The shading of the images reflects the surface topography (z) and was maintained in the different images that are being compared: Figs. 2A, 2B, 2C, and 3A; Figs. 2D, 2E, and 3B.
18. B. Vollmert, *Polymer Chemistry* (Springer-Verlag, New York, 1973); A. G. Walton and J. Blackwell, *Biopolymers* (Academic Press, New York, 1973).
19. The individual polymer molecules may be oriented along the scan direction, as one would generally expect. However, the formation of the aggregates is quite rapid and we were unable to resolve the orientation of the individual polymer molecules within the bundles.
20. We were unable to produce oriented bundles in polyethylene oxide, which was deposited from crystallites; rather, we saw small crystalline structures similar to those observed with optical and electron microscopes. Furthermore, if we reduced the operating force by imaging polystyrene film deposited on mica under water, the interaction between the tip and the polymer was reduced, and we were unable to produce the alignment.

21. This work was supported in part by the Natural Science and Engineering Research Council of Canada. We thank M. Moskovits and T. Dickson for helpful discussions and reading of the manuscript.

8 August 1991; accepted 31 October 1991

Luminescent Colloidal Silicon Suspensions from Porous Silicon

JULIE L. HEINRICH, CORRINE L. CURTIS, GRACE M. CREDO, KAREN L. KAVANAGH,* MICHAEL J. SAILOR*

A procedure for generating colloidal suspensions of Si that exhibit luminescence, attributed to quantum confinement effects, is described. Samples of *n*- or *p*-type Si that have been electrochemically etched to form porous Si can be ultrasonically dispersed into methylene chloride, acetonitrile, methanol, toluene, or water solvents, forming a suspension of fine Si particles that luminesce. Transmission electron microscopy analyses show that the Si particles have irregular shapes, with diameters ranging from many micrometers to nanometers. Luminescent, composite polystyrene/Si films can be made by the addition of polystyrene to a toluene suspension of the Si nanoparticles and casting of the resulting solution onto a glass slide.

SMALL COLLOIDAL SEMICONDUCTOR particles (typically ~10 nm in diameter) have properties that deviate substantially from those of the bulk material. As the particle size in semiconductors approaches the exciton diameter, the particles are referred to as quantum-size particles (*1–3*). A number of colloidal semiconductors exhibiting quantum confinement effects in either their emission or their absorption spectra have been synthesized, including Si (*4, 5*),GaAs (*6, 7*), and many of the I-VII and II-VI semiconductors (*2*). The study of

J. L. Heinrich, C. L. Curtis, G. M. Credo, M. J. Sailor, Department of Chemistry, The University of California at San Diego, La. Jolla, CA 92093.
K. L. Kavanagh, Department of Electrical and Computer Engineering, The University of California at San Diego, La Jolla, CA 92093.

*To whom correspondence should be addressed.

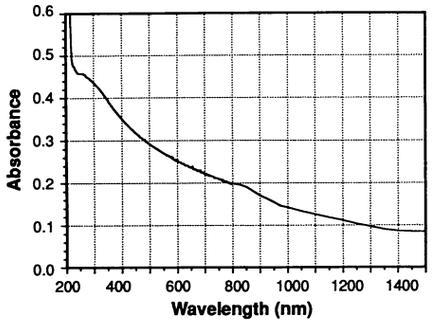

Fig. 1. Absorption spectrum of an *n*-Si suspension in acetonitrile versus an acetonitrile background. The solution contains approximately 0.1 mg of Si per milliliter. Path length is 1 cm.

these systems is becoming more important as the technology for producing very small electronic circuitry approaches the quantum-size regime in more than one dimension. In addition, the photochemical and nonlinear optical properties of such materials are of interest for their potential technological applications (*8–10*). Colloidal semiconductors exhibiting quantum confinement effects have been prepared in solution (*1–3*), polymer (*11*), glass (*12*), and zeolite (*13*) matrices. Fundamental studies of semiconductor particles in solution have yielded information about the surface chemistry of semiconductors, the chemical properties of defects, and the details of interfacial charge transport (*14–23*).

For the technologically important semiconductor Si, quantum-size particles have been synthesized from silane via slow combustion (*4*), microwave plasma (*5*), or chemical vapor deposition (*24*). These preparations produce impure Si crystallites that contain a large amount of SiO_2. Recently, quantum-size Si has been prepared from electrochemically etched single-crystal Si wafers ("porous Si") (*25–27*). Because it is prepared in an HF electrolysis bath, the resulting Si material has a clean, H-terminated surface that contains no SiO_2 (*28, 29*). We report here that colloidal suspensions of Si can be prepared in a variety of solvents by the ultrasonic dispersion of electrochemically etched Si wafers. In contrast to the gas-phase preparations of colloidal Si, this technique produces Si particles from high-purity semiconductor-grade substrates, resulting in a more convenient synthesis that avoids contamination by SiO_2 and other impurities. This method of preparation opens up a new area of study for luminescent porous Si and provides greater options for exploiting its properties. In a demonstration of the latter, we have characterized composite Si/polystyrene films fabricated from an Si suspension in toluene. The solutions and the polymer films display visible luminescence characteristic of quantum-size Si.

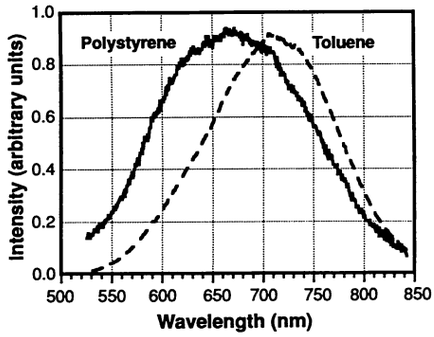

Fig. 2. Emission spectra of Si particulates in a toluene suspension (dashed line) and in a polystyrene film (solid line). The polystyrene film was cast from a toluene suspension of *n*-Si particulates.

Single-crystal polished (100) wafers of P-doped (*n*-type) Si of 0.5 to 2 ohm-cm resistivity and B-doped (*p*-type) Si of 6 to 10 ohm-cm resistivity were used. Ohmic contacts were formed as previously described (*30*) and mounted such that only Si was exposed to the etching bath. The resulting Si electrode was used as the working electrode in a two-electrode electrochemical cell. A Pt sheet was used as the counterelectrode. The etching bath was a 50:50 (by volume) solution of aqueous HF (Fisher Scientific, Electronic grade) and 95% ethanol (Quantum Chemical Company). The *n*-Si samples were held at 0.0 V with respect to the Pt counterelectrode, and the current density was adjusted by illuminating with a 300-W tungsten (ELH) lamp. The *p*-Si samples were held at potentials ranging from 0.6 to 1.6 V versus the Pt counterelectrode. We produced luminescent porous Si by galvanostatically etching either *n*- or *p*-Si at current densities between 0.1 and 5 mA/cm^2 for 1 hour (*n*-Si) or 6 hours (*p*-Si). The samples were then removed from the bath, rinsed with water, and air-dried. In contrast to previous reports that a subsequent slow etch is necessary to produce luminescent porous Si (*26, 27*), we observed visible luminescence immediately upon removal of the samples from the electrochemical etch. The luminescence is visible to the naked eye as a red-orange to yellow glow when the samples are illuminated with a small ultraviolet (UV) lamp (Mineralight UVS-II). The primary difference between the present etching technique and that used in earlier reports (*26*) is the anodic current density, which is lower in the present work. For the *n*-type samples, we found that the intensity of emission could be increased by following the initial slow etch with a short (20 s) etch at 100 mA/cm^2. Infrared (IR) spectra of the anodized wafers displayed

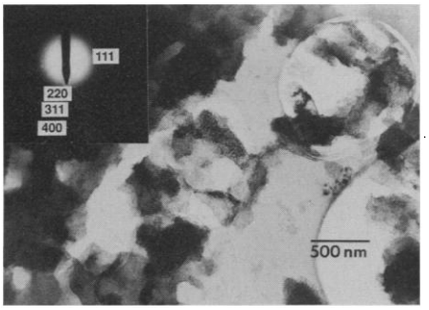

Fig. 3. Bright-field transmission electron micrograph of a cluster of Si particles on a polystyrene-coated Cu grid taken at an accelerating voltage of 300 kV. The selected area diffraction pattern (inset) shows a polycrystalline ring pattern characteristic of Si.

strong Si–H stretches in the 2050 to 2150 cm^{-1} region and lacked discernible peaks for surface Si–O, indicative of the clean, H-terminated Si surface characteristic of freshly etched porous Si (*28, 29*).

From this point on, we carried out all manipulations under a dry N_2 atmosphere, using purified, dried solvents with conventional Schlenk and syringe techniques (*31*). In a typical preparation, 10 ml of solvent were added to a flask containing the anodized Si wafer and the mixture was placed in a Fisher Scientific FS5 ultrasonic cleaning bath for between 15 min and 2 hours. We monitored the dissolution of the porous Si periodically by observing the luminescence of the solution upon irradiation with a UV lamp. After removal from the ultrasonic bath the solution was allowed to settle for 1 hour, and the supernatant was removed from the settled solids. We made flexible, transparent films of the composite Si/polystyrene by adding polystyrene to a toluene suspension of Si particles and then casting the resulting solution onto a glass slide in air.

The UV–visible–near-IR absorption spectrum of a representative colloid solution (in acetonitrile) (Fig. 1) was similar to the published spectrum of Si particles synthesized from silane combustion (*4*). The emission spectrum of a suspension in toluene was obtained with a charge-coupled device detector (0.25-m monochromator, liquid N_2-cooled) (Fig. 2). The excitation source was the defocused 442-nm line of a 10-mW He/Cd laser. The maximum wavelength λ_{max} of emission varied between 750 and 650 nm for different solvent preparations, and the peak width at half maximum was typically 200 nm. These emission spectra qualitatively match those of the solid samples before dissolution, as well as those obtained on plasma-deposited Si nanoparticles (*5*).

The emission spectrum of an Si/polystyrene film was also taken (Fig. 2). The lumi-

nescence is visible to the naked eye, although it is noticeably less intense and shifted to higher energy with respect to the emission spectrum of the parent (non–polymer-containing) Si dispersion in toluene. This shift is attributed to oxidation of the Si particles during the casting process. Similar shifts in the emission spectra have been observed upon exposure of porous Si to air (*32*). The pure toluene and polystyrene films showed no detectable luminescence.

Transmission electron microscope (TEM) images were obtained by pipetting a drop of the Si colloidal suspension onto the middle of a polystyrene-dipped TEM grid (Cu mesh) in air. In the microscopy we used a Philips CM30 TEM at an acceleration voltage of 100 or 300 keV. Si particles attached to thin regions and near holes in the polystyrene could be studied (Fig. 3). Crystalline, overlapping Si particles are clearly visible against an amorphous polystyrene background. The particles are irregularly shaped and range in size from many micrometers down to the resolution limit of the TEM (about 0.2 nm). This image is consistent with the known structural properties of bulk porous Si as seen from TEM and scanning electron microscopy (*33–35*). The inset shows a selected area diffraction pattern clearly identifiable as polycrystalline Si. The edges of each particle and the smallest particles are very thin, less than 10 nm thick. Convergent beam diffraction showed these regions to be predominantly amorphous, although TEM images of luminescent porous Si have recently been reported showing small crystalline regions (*36*). The lack of crystallinity observed in the present work is possibly the result of oxidation during exposure to air or electron beam damage during microscopy. Presumably the smaller particles and the thin regions on the larger particles are responsible for the luminescence observed in these samples, as quantum confinement effects are expected to appear in Si particles no larger than several nanometers (*1–3*).

REFERENCES AND NOTES

1. A. Henglein, *J. Chim. Phys. Physicochim. Biol.* **84**, 1043 (1987).
2. ———, *Chem. Rev.* **89**, 1861 (1989).
3. L. Brus, *J. Phys. Chem.* **90**, 2555 (1986).
4. A. Fojtik, H. Weller, S. Fiechter, A. Henglein, *Chem. Phys. Lett.* **134**, 477 (1987).
5. H. Takagi, H. Ogawa, Y. Yamazaki, A. Ishizaki, T. Nakagiri, *Appl. Phys. Lett.* **56**, 2379 (1990).
6. C. J. Sandroff *et al.*, *Science* **245**, 391 (1989).
7. M. A. Olshavsky, A. N. Goldstein, A. P. Alivisatos, *J. Am. Chem. Soc.* **112**, 9438 (1990).
8. Y. Wang, *Acc. Chem. Res.* **24**, 133 (1991).
9. R. Jain and R. Lind, *J. Opt. Soc. Am.* **75**, 647 (1983).
10. R. A. Morgan, S.-H. Park, S. W. Koch, N. Peyghambarian, *Semicond. Sci. Technol.* **5**, 544 (1990).
11. Y. Wang, A. Suna, W. Mahler, R. Kasowski, *J. Chem. Phys.* **87**, 7315 (1987).
12. T. Rajh, M. I. Vucemilovic, N. M. Dimitrijevic, O. I. Micic, A. J. Nozik, *Chem. Phys. Lett.* **143**, 305 (1988).
13. Y. Wang and N. Herron, *J. Phys. Chem.* **91**, 257 (1987).
14. T. Dannhauser, M. O'Neil, K. Johansson, D. Whitten, G. McLendon, *ibid.* **90**, 6074 (1986).
15. C.-H. Fischer and A. Henglein, *ibid.* **93**, 5578 (1989).
16. S. Gallardo, M. Gutierrez, A. Henglein, E. Janata, *Ber. Bunsenges. Phys. Chem.* **93**, 1080 (1989).
17. M. Haase, H. Weller, A. Henglein, *J. Phys. Chem.* **92**, 482 (1988).
18. D. Hayes, O. I. Micic, M. T. Nenadovic, V. Swayambunathan, D. Meisel, *ibid.* **93**, 4603 (1989).
19. P. V. Kamat, T. W. Ebbesen, N. M. Dimitrijevic, *Chem. Phys. Lett.* **157**, 384 (1989).
20. D. Meisel and W. A. Mulac, *Coll. Surf.* **35**, 179 (1989).
21. M. O'Neil and G. McLendon, *Chem. Phys. Lett.* **147**, 565 (1988).
22. L. Spanhel, M. Haase, H. Weller, A. Henglein, *J. Am. Chem. Soc.* **109**, 5649 (1987).
23. Y. Wang and N. Herron, *J. Phys. Chem.* **91**, 5005 (1987).
24. D. J. DiMaria *et al.*, *J. Appl. Phys.* **56**, 401 (1984).
25. V. Lehmann and U. Gosele, *Appl. Phys. Lett.* **58**, 856 (1990).
26. L. T. Canham, *ibid.* **57**, 1046 (1990).
27. A. Halimaoui *et al.*, *ibid.* **59**, 304 (1991).
28. T. Ito, H. Kiyama, T. Yasumatsu, H. Watabe, A. Hiraki, *Physica B* **170**, 535 (1991).
29. P. Gupta, V. L. Colvin, S. M. George, *Phys. Rev. B* **37**, 8234 (1988).
30. N. S. Lewis, *J. Electrochem. Soc.* **131**, 2496 (1984).
31. D. F. Shriver and M. A. Drezdzon, *The Manipulation of Air-Sensitive Compounds* (Wiley, New York, 1986).
32. L. T. Canham, M. R. Houlton, W. Y. Leong, C. Pickering, J. M. Keen, *J. Appl. Phys.* **70**, 422 (1991).
33. M. D. Drory, P. C. Searson, L. Liu, *J. Mater. Sci. Lett.* **10**, 81 (1991).
34. S. F. Chuang, S. D. Collins, R. L. Smith, *Appl. Phys. Lett.* **55**, 1540 (1989).
35. G. Bomchil and A. Halimaoui, *Appl. Surf. Sci.* **41/42**, 604 (1989).
36. A. G. Cullis and L. T. Canham, *Nature* **353**, 335 (1991).

37. The work of G.M.C. was supported by the NSF Young Scholars Program.

9 September 1991; accepted 5 November 1991

Strontium Isotopic Composition of Estuarine Sediments as Paleosalinity-Paleoclimate Indicator

B. L. INGRAM AND D. SLOAN

The strontium isotopic composition of biogenic precipitates that occur in estuarine sediments can be used as proxy indicator of paleosalinity and for assessing precipitation and river discharge rates over thousands of years. In the San Francisco Bay estuary, river water with low $^{87}Sr/^{86}Sr$ ratio (average, 0.7065) and low Sr concentration (0.13 parts per million) mixes with seawater with a higher $^{87}Sr/^{86}Sr$ ratio (0.7092) and Sr concentration (7.9 parts per million). The predicted mixing relation between salinity and Sr isotopic composition is confirmed by measurements of modern estuarine surface waters. A paleosalinity record obtained from foraminifera for the ancestral San Francisco Bay during oxygen isotope substage 5e of the last interglacial reflects a global rise and fall of sea level, and short time-scale variations related to fluctuations in discharge rates of the Sacramento and San Joaquin rivers.

ESTUARIES ARE GEOLOGICALLY short-lived features, existing mainly during times of relatively high sea level; but, because estuaries are sensitive to climatic changes, the geochemistry and faunal assemblages in estuarine sediments are an important source of paleoclimatic and paleohydrologic information. In this paper, we describe a geochemical method of determining paleosalinity of estuarine waters and report results obtained from San Francisco Bay, the largest estuarine system on the west coast of North America, for oxygen isotope substage 5e of the last interglacial (about 120,000 years before present). As San Francisco Bay receives freshwater from 40% of the surface area of California (162,000 km^2) by way of the Sacramento and San Joaquin rivers and their tributaries (Fig. 1) (*1*), salinity variations in the geologic record provide a proxy for precipitation and runoff from a large continental area. Because streamflow in the western United States and Hawaii reflects large-scale North Pacific winter atmospheric circulation, the Sr isotopic data may have broad paleoclimatic and paleohydrologic implications (*2*).

The salinity of San Francisco Bay water is a function of freshwater inflow rates and sea level; the latter controls the entry of saline (33 to 35 per mil) ocean water into the bay through the Golden Gate (Fig. 2) (*1, 3*). The inflow of freshwater is seasonal; maximum river discharge occurs during winter and early summer, reflecting winter rains and spring snowmelt (*1*). Because most of the state's annual precipitation falls in northern California, 80% of the freshwater enter-

B. L. Ingram, Department of Geology, Stanford University, Stanford, CA 94305, and Berkeley Center for Isotope Geochemistry, Department of Geology and Geophysics, University of California, Berkeley, CA 94720. D. Sloan, Museum of Paleontology, University of California, Berkeley, CA 94720.